UCRL-JC-119032
PREPRINT

The Opal Opacity Code: New Results

F. J. Rogers
C. A. Iglesias

This paper was prepared for submittal to the
Proceedings of the Astronomical Society of the Pacific Conference Series
Hague, The Netherlands
August 15-27, 1994

August 1994

Lawrence Livermore National Laboratory

This is a preprint of a paper intended for publication in a journal or proceedings. Since changes may be made before publication, this preprint is made available with the understanding that it will not be cited or reproduced without the permission of the author.

DISCLAIMER

This document was prepared as an account of work sponsored by an agency of the United States Government. Neither the United States Government nor the University of California nor any of their employees, makes any warranty, express or implied, or assumes any legal liability or responsibility for the accuracy, completeness, or usefulness of any information, apparatus, product, or process disclosed, or represents that its use would not infringe privately owned rights. Reference herein to any specific commercial product, process, or service by trade name, trademark, manufacturer, or otherwise, does not necessarily constitute or imply its endorsement, recommendation, or favoring by the United States Government or the University of California. The views and opinions of authors expressed herein do not necessarily state or reflect those of the United States Government or the University of California, and shall not be used for advertising or product endorsement purposes.

THE OPAL OPACITY CODE: NEW RESULTS

Forrest J. Rogers and Carlos A. Iglesias

Lawrence Livermore National Laboratory, P. O. Box 808, Livermore, Ca 94550, USA

ABSTRACT The OPAL code was developed to calculate the wide range of frequency-dependent and mean opacity data needed to model laboratory experiments and stellar interiors. We use parametric potentials to generate vastly more atomic data than used in earlier opacity work for all elements with atomic number less than 35. We have also developed an improved equation of state based on an activity expansion of the grand canonical partition function. We give herein a brief description of the OPAL code and present new results that include the effect of additional heavy elements compared to our earlier calculations. The importance of very heavy elements having atomic number greater than 30 is also discussed. We present some comparisons with recent results from the Opacity Project and some directions for future work.

1. INTRODUCTION

Renewed interest in theoretical opacities has been driven by the rapid increase in the breadth and quality of stellar observations in recent years. In a number of cases stellar models have failed to provide satisfactory explanations of the observations. The most widely known example has been attempts to explain the solar neutrino production rate. This, plus a number of other stellar properties that could not be adequately explained by theoretical models were known to be sensitive to the opacity. It was noticed that arbitrarily increasing the opacity in the few hundred-thousand degree temperature range by factors of 2-3 would improve some calculated properties of variable stars (Fricke, Stobbie, and Strittmatter 1971; Petersen 1974; Stellingswerf 1978; Simon 1982), increasing the opacity by about 40% at slightly higher temperatures would improve the calculated Li abundance in the Hyades cluster (Swenson, Stringfellow, and Faulkner 1990), and increasing the opacity by 10-20% around a few million degrees would improve the predicted solar p-mode frequencies (Christensen-Dalsgaard *et al.* 1985; Korzenik and Ulrich 1989; Cox *et al.* 1989).

The primary source of opacity data from the early 1960's until recently has been the Los Alamos National Laboratory (Cox and Stewart 1962; Cox and Tabor 1976; Huebner *et al.* 1977). These were the first extensive calculations to include bound-bound absorption and they were quite successful at explaining the main features of stellar evolution. St. Andrews University has also provided opacity data (Carson, Mayers, and Stibbs 1968; Carson 1976). In response to a plea by Simon (1982) to reinvestigate the opacity, Magee *et al.* (1984) concluded that uncertainties in the existing Los Alamos data were around 20% and rejected the possibility of large increases in the theoretical opacity.

Due to the importance of radiation transport for a wide range of stellar problems, two groups undertook completely new, independent efforts to calculate

astrophysical opacities. One of these, known as the Opacity Project (OP), is an international collaboration concerned with stellar envelopes. The other, known as OPAL and located at the Lawrence Livermore National Laboratory, is concerned with the full range of interior opacities needed in stellar modeling. Contrary to the conclusions of Magee *et al.* (1984), preliminary OPAL results showed substantial increases in opacity (Iglesias, Rogers, and Wilson 1987) and up to factors of four have been reported in more complete calculations (Iglesias and Rogers 1991; Rogers and Iglesias 1992a; Iglesias, Rogers, and Wilson 1992a; Seaton *et al.* 1994). These increases are largely due to the rich spectrum of transitions originating in partially-ionized iron with an important contribution from the intra M-shell transitions neglected by Los Alamos.

2. ROSSELAND MEAN OPACITY

The radiation transfer equation describes the transport of energy by photons and is equivalent to the Boltzmann equation in the kinetic theory of particle transport (Mihalas 1978). For steady-state conditions it is given by

$$\frac{dI_\nu(s,\mathbf{n})}{ds} = -\kappa_\nu I_\nu(s,\mathbf{n}) + j_\nu \tag{1}$$

where $I_\nu(s, \mathbf{n})$ is the intensity at frequency ν in the direction $\mathbf{n}$ as a function of distance s, and j_ν is the emissivity. The monochromatic opacity, κ_ν, is given by

$$\kappa_\nu = (1 - e^{-h\nu/kT})\Sigma_i \chi_i \left\{ \kappa_i^{bb} + \kappa_i^{bf} + \kappa_i^{ff} \right\} + \kappa^s, \tag{2}$$

where the sum is over elements in the mixture, χ_i is the number fraction, κ^{bb}, κ^{bf}, and κ^{ff}, are the bound-bound, bound-free, and free-free absorption cross-sections, respectively, κ^s is the scattering cross-section and the factor [1-exp($h\nu/kT$)] accounts for stimulated emission.

Conditions inside a star are close to local thermodynamic equilibrium so that according to Kirchhoff's law,

$$j_\nu = \kappa_\nu B_\nu(T), \tag{3}$$

where,

$$B_\nu = (2h\nu^3 / c^2)(e^{h\nu/\kappa T} - 1)^{-1} \tag{4}$$

is the Planck function. In addition, conditions change slowly over many photon mean-free paths and the radiation transfer equation greatly simplifies. In this limit, known as the diffusion approximation, κ_ν can be replaced with a flux weighted harmonic mean according to

$$\frac{1}{\kappa_R} = \int_0^\infty d\nu \frac{1}{\kappa_\nu} \frac{dB_\nu}{dT} \Bigg/ \int_0^\infty d\nu \frac{dB_\nu}{dT} \quad . \tag{5}$$

In Eq. (5) κ_R is the Rosseland mean opacity or simply the opacity. A large value of the opacity indicates strong absorption from a beam of photons, whereas a small value indicates that the beam loses very little energy as it passes through the medium.

3. THE OPAL CODE

It was apparent from the beginning that the most computationally intensive part of developing a new opacity code would be the vast amount of bound-bound and bound-free absorption cross-sections required in the calculations. Several levels of detail for including atomic data are possible. For example, consider transitions that connect two electrons in an *sp* configuration to a p^2 configuration through a one electron jump. In the simplest approximation the transitions are degenerate. Opacity calculations that carry out a sum over transitions in this approximation are referred to as detailed configuration accounting (DCA) methods. However, the DCA approach neglects non-spherical interactions that remove the degeneracy and lead to configuration term structure. In light elements the dominant non-spherical term is the Coulomb interaction between electrons which leads to pure LS coupling. In LS coupling the single spectral line of the DCA method in our example splits into three distinct lines corresponding to a triplet and two singlet terms. With heavier elements, such as those in the iron group, the interaction between the electron spin and the magnetic field resulting from the electron orbital motion is no longer negligible and requires intermediate coupling (Cowan 1981). In intermediate coupling the three lines in LS coupling split into eight lines having no net total spin change, $\Delta S=0$, and 6 intercombination lines having $\Delta S=\pm 1$. In more complicated configurations the increase in the number of spectral lines can be more dramatic.

Stellar opacities require detailed atomic data for arbitrary configurations and ion stages for all elements in an astrophysical mixture. To calculate the required atomic data we developed a parametric potential method that is fast enough to allow on-line calculations, while achieving accuracy comparable to single configuration Dirac-Fock results (Rogers, Wilson , and Iglesias 1988). This on-line capability also provides flexibility to study easily the effects of atomic physics approximations such as various angular momentum couplings or data averaging methods. For example, the large increase in the iron opacity obtained with the LS coupling scheme compared to calculations that neglect term splitting were an indication that fine structure should also be included (Rogers and Iglesias 1992a). As a result, more recent OPAL calculations include the spin-orbit effect in full intermediate coupling (Iglesias, Rogers, and Wilson 1992a).

By contrast, the OP group uses first principle methods to construct detailed atomic databases that include configuration interactions in the bound-bound and bound-free cross-sections. Furthermore, the OP atomic data has been archived and is available for other types of investigations (Cunto *et al.* 1993). Note that configuration-interaction is most important for neutral and near neutral atoms and ions. Although the OP atomic data was computed with LS coupling, an approximate

method that neglects spin changing transitions was developed to include fine structure in the opacity calculations (Seaton *et al.* 1994). The available Los Alamos opacity data is mostly in the DCA approximation, but more detailed calculations are in progress (Magee 1993; Magee *et al.* 1994).

3.1. Parametric Potentials

When discussing the parametric potentials in OPAL, it is convenient to define an electron configuration as having two components. The first component is a "parent" configuration consisting of all electrons in a given configuration except one. The excluded electron defines the second component or "running" electron. The parent configuration defines the potential for all subshells and scattering states available to the running electron. In order to incorporate the shell structure of the parent configuration, Rogers (1981a) introduced a potential with a Yukawa term for each occupied shell in the parent configuration,

$$V(r) = -\frac{2}{r}\left[(Z-\nu) + \sum_{n=1}^{n^*} N_n\, e^{-\alpha_n r}\right] \tag{6}$$

(in Rydbergs), where

$$\nu = \sum_{n=1}^{n^*} N_n \tag{7}$$

is the number of electrons for a parent ion, N_n the number of electrons in the shell with principal quantum number n, n^* the maximum value of n for the parent configuration, and α_n the screening parameter for the electrons in shell n. The screening parameters in Eq. (6) are determined by iteratively solving a spin-averaged Dirac equation and matching the eigenvalues to the experimentally deduced one electron configuration-averaged ionization energies.

At this point, it is useful to discuss an example. Consider the configuration $1s^2 2s^2 2p^4$. For the ionization of a 2p electron, the system is defined by the parent $1s^2 2s^2 2p^3$ plus a running electron. In fact, this parent describes all transitions of the form

$$1s^2 2s^2 2p^3 n_1 l_1 \quad \text{to} \quad 1s^2 2s^2 2p^3 (n_1 l_1)' \quad \text{or to} \quad 1s^2 2s^2 2p^3 \varepsilon l_1'$$

where $n_1 l_1$ and $(n_1 l_1)'$ denote the set of orbitals 2p, 3s, 3p, ... and ε the energy of the scattering states, so that photoionization and bremsstrahlung can be considered. Similarly the parent $1s2s^2 2p^4$ describes transitions of the form

$$1s2s^2 2p^4 n_2 l_2 \quad \text{to} \quad 1s2s^2 2p^4 (n_2 l_2)' \quad \text{or to} \quad 1s2s^2 2p^4 \varepsilon l_2'$$

where now $n_2 l_2$ includes the 1s but not the 2s orbital.

If we assign n_1l_1=2p and n_2l_2=1s in the examples above, then the initial configurations are identical. However, it is important to note that the effective potentials are different since the parent configurations are different. In contrast, a self-consistent field (SCF) potential uses the same set of orbital wave functions for the initial configurations in both sets of transitions above. It follows that the effective potential is not an independent particle parametrization of a SCF potential. In OPAL, transition energies are assumed to be differences between eigenvalues of the running electron. The eigenvalues of the parent-configuration closed shells have no physical interpretation. In contrast, the interpretation in SCF eigenvalues as ionization energies (neglecting orbital relaxation) is a consequence of Koopmans' theorem.

The simplest configurations involve a closed core plus an open valence subshell for which there exists good experimental data. Screening parameters are obtained systematically for each isoelectronic sequence. Starting with two electron ions (one electron parents), a spin-averaged Dirac equation was solved iteratively to find the screening parameter for the K-shell that best reproduces experimental ground configuration ionization energies. The procedure continues by adding one electron to the parent configuration at a time. Note that matching the experimental energies is simplified since the parameters for the inner shells are fixed at the closed shell value and only the outer-most shell screening parameter is optimized.

Each shell parameter can be fitted accurately along an isoelectronic sequence with the simple form

$$\alpha_n = \left(\xi_n + 1\right) \sum_{j=0}^{3} \frac{a_j(\nu_n)}{\xi_n^j}. \tag{8}$$

The screening parameters are fitted by coefficients that depend on

$$\nu_n = \sum_{n=1}^{n} N_n \qquad \text{and} \qquad \xi_n = Z - \nu_n, \tag{9}$$

where ν_n is the occupancy of the parent up to shell n and ξ_n the net charge at that shell for the parent-configuration ion. The resulting set of a_j's in Eq. (8) is relatively small and is given in Rogers, Wilson, and Iglesias (1988).

These one-open valence shell configurations comprise only a small subset of all the transitions that must be considered in an opacity calculation. For example, configurations involving inner shell excitations (underlined subshells indicate running electron jumps)

$$\underline{1s}^2 2s^2 2p^2 \quad \text{to} \quad 1s2s^2 2p^2 \underline{n}\underline{p} \quad \text{and} \quad 1s^2 \underline{2s}^2 2p^2 \quad \text{to} \quad 1s^2 2s2p^2 \underline{n}\underline{p}.$$

must be included. Multiply excited configurations also need to be considered,

$$1s^2 2s^2 \underline{2p} nl \quad \text{to} \quad 1s^2 2s^2 nl\,(\underline{nl})' \quad \text{and} \quad 1s^2 \underline{2p}^4 \quad \text{to} \quad 1s^2 2p^3 \underline{nl}$$

and, of course, combinations of the above

$1s^2\underline{2s}^2 2pnl$ to $1s^2 2s2pnl(\underline{nl})'$.

In these examples (as well as in the parametric potential model) the atomic structure is described by single configurations when obviously a very accurate description would require configuration interactions. Although this may appear to be a limitation of the approach, in particular when comparing to spectroscopic data, for opacity calculations it does not seem to be an issue. On the flip side of the coin, approaches based on atomic structure calculations which have configuration interactions must be certain to include the vast amounts of necessary data. Probably the optimal approach would be accurate data bases supplemented by quick, reasonably accurate methods such as parametric potentials to obtain a complete data set.

It was shown in Rogers, Wilson, and Iglesias (1988) how it is possible to generate from the simpler one-open valence shell parent configurations screening parameters for more complicated situations such as multiply excited ions and inner core excitations. The procedure involves simple scaling laws based on physical arguments. In deriving the scaling laws it was necessary to resort to atomic structure codes since for these more complicated configurations experimental data is limited.

The parametric potentials in Eq. (6) provide the configuration-average energies and a set of radial wave functions, $\{\psi_{nl}\}$. In order to obtain reasonable agreement with spectral data, it is necessary to consider the energy level structure of configurations. In OPAL, the calculation is done in the single-configuration approximation of the Slater-Condon theory of atomic structure (Cowan 1981). The term energies can be obtained using Racah algebra and involve Slater integrals which in turn depend on the set $\{\psi_{nl}\}$. As mentioned above, the one-electron binding energies for each subshell of a configuration is computed from a distinct parent-configuration effective potential. Consequently, the set $\{\psi_{nl}\}$ to be used in the configuration structure calculation is not uniquely defined. For simplicity, $\{\psi_{nl}\}$ is chosen from the parent associated with both initial and final configurations of a given transition. For example, for the transition $1s^2 2s2p^2$ to $1s^2 2p^2 3p$ where the running electron makes a 2s to 3p jump, the appropriate parent configuration is $1s^2 2p^2$.

Calculations with the parametric potentials, which accurately reproduce ionization energies, do not *a priori* guarantee accurate oscillator strengths since these quantities involve expectation values that weight different regions of the radial wave functions. Furthermore, photoionizations cross sections require scattering states and again there is no *a priori* reason for these to be accurate. Nevertheless, the parametric potentials model both the long-range and inner structure of atoms for both discrete and continuum states and the resulting photoabsorption cross sections are comparable to SCF calculations (Rogers, Wilson, and Iglesias 1988). Comparisons with OP and experiment are given in Iglesias, Rogers, and Wilson (1992b).

3.2. Modeling of Laser Experiments

Comparisons with transmission measurements of laser produced plasmas provide a stringent test of calculations involving large amounts of atomic data. Figure 1 shows an OPAL transmission calculation for an Al-Nb sample using the parametric potentials compared to experiment (Springer e*t al.* 1991). The absorption in this photon energy region is mostly due to n=1 to 2 transitions in Al. Figure 2 shows the same comparison but now the atomic data in the calculation was generated with a multi-configuration Dirac Fock code (Chen 1985). Both calculations do a good job,

but the MCDF atomic data is clearly superior. The largest discrepancy using the parametric potentials is the strong feature at 1575 eV not present in the experiment. The good news for opacity calculations is that the Rosseland integral over the energy range of the experiment is almost identical for both sets of calculations. Consequently, we use the computationally fast parametric potential method to calculate Rosseland mean opacities and the MCDF method to model experiments.

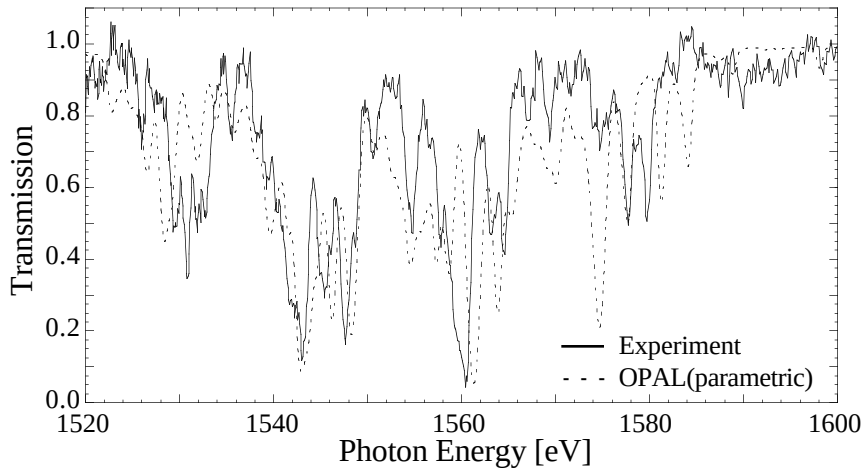

FIG. 1 Comparison of transmission experiment and OPAL calculations using parametric potentials for an Al-Nb mixture with T=49eV and ρ=0.0257g/cm^3 assuming an experimental energy resolution of 0.75eV.

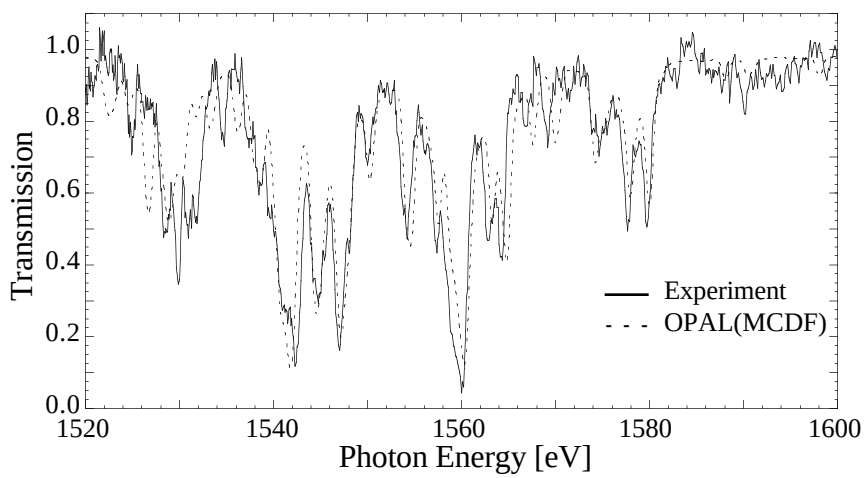

FIG. 2 Same as Fig. 1 with MCDF atomic data in the OPAL calculations.

3.3. Equation of State

The equation of state plays an important role in opacity calculations by providing the occupation numbers needed to evaluate Eq. (2). The OP and OPAL equation of state approaches are quite different, but for typical stellar conditions give very similar thermodynamic results (Däppen 1992). However, the predicted occupation numbers are different for highly excited states that can affect the opacity at high density; the OPAL values being somewhat larger. The OP calculation is based on a free energy minimization, or chemical picture (Hummer and Mihalas 1988), whereas the OPAL calculation is based on activity expansions of the grand canonical ensemble, or physical picture (Rogers 1981b).

The OPAL approach treats the system in terms of its fundamental constituents, electrons and nuclei. The procedure is to expand the pressure as a sum of two-body, three-body terms, etc. (i.e., a cluster expansion). However, the long range of the Coulomb potential introduces substantial complications. In addition, the quantum nature of electrons introduces degeneracy and exchange corrections. The attractive electron-ion interaction leads to short distance divergences in classical cluster coefficients so that quantum mechanics is essential. The activity expansion method takes advantage of graphical resummation procedures to remove the long-range divergences occurring in all cluster coefficients of plasmas. Composite particles (ions, atoms, and molecules) arise naturally in the physical picture and plasma effects on the bound states are determined from theory (Rogers 1986; 1989; 1994). This is a definite advantage over current chemical picture methods which must introduce intuitive models to obtain these effects. The approach also provides systematic procedures for including higher order Coulomb corrections. Detailed descriptions of the activity expansion methods can be found in Ebeling *et al.* (1976); Rogers (1981b); Kraeft *et al.* (1986).

3.4. Additional Details

The OPAL calculations include degeneracy and plasma collective effects in the free-free absorption using a screened form of the parametric potentials, whereas these effects are not currently included in OP. In both OPAL and OP collective effects on the Thomson scattering are obtained from the method of Boercker (1987). In OPAL spectral line broadening for one, two, and three electrons ions are obtained from a suite of codes provided by Lee (1988) that include linear Stark theory. For all other transitions the OPAL calculations use Voigt profiles where the Gaussian width is due to Doppler broadening and the Lorentz width includes natural plus electron impact collision broadening (Dimitrievic and Konjevic 1980). The source of the largest opacity increases has been improved atomic physics, but improved equation of state and line broadening have also been important.

4. OPAL OPACITIES

Accurate models of stellar structure require detailed computer calculations. However, in regions where radiation pressure dominates, the ratio of the matter pressure to the radiation pressure is approximately constant (Bohm-Vitense 1992). Using the non-relativistic ideal gas pressure in combination with the Stefan-Boltzmann law, one obtains with the above assumption a constant value for density/(temperature)^3. Thus, it is convenient to tabulate the Rosseland mean opacity

at constant values of $R=\rho/T_6^3$,where ρ is the material density in g/cm^3 and T_6 is the temperature in units of million of degrees.

A large number of calculations have been reported using OPAL opacities (e.g., Rogers and Iglesias 1994). For example, pulsation instabilities for β-Cephei stars as actually observed are now predicted (Cox *et al.* 1992: Kiriakidis, El Eid, and Glatzel 1992; Moskalik and Dziembowski 1992) and calculated period ratios for double mode classical Cepheids and RR-Lyrae stars agree closely with observations at evolutionary masses (Kovacs, Buchler and Marom 1992; Cox 1991; Moskalik, Buchler and Marom 1992). In addition, the location of stellar models in the observational planes relating mass, luminosity, effective temperature, and radius is substantially improved for main-sequence stars (Stothers and Chin 1991; 1993); the observed lithium abundance of stars in the Hyades cluster can be modeled without invoking exotic theories (Swenson *et al.* 1994); the computed solar seismic frequencies as well as the inner boundary radius of the solar convection zone are in close agreement with observations (Dziembowski, Pamyatnykh, and Sienkiewicz 1992; Guenther *et al.* 1992; Bahcall and Pinsonnealt 1992; Cox and Guzik 1993); and the calculated light curves for the decay phase of classical novae agree better with observation (Kato 1994).

4.1. Comparison with Cox and Tabor

Figure 3 shows opacity as a function of temperature at constant logR=-3. OPAL results are displayed for mixtures with hydrogen mass fraction X= 0.7 and metal mass fraction Z=0 and 0.02. The helium mass contents are, thus, Y=0.3 and 0.28, respectively. The results for the commonly used Cox and Tabor (1976) opacities with Z= 0.02 are also plotted. The curves show a series of bumps in log κ_R that are due to strong absorption features in the spectrum of the indicated species. The H, He and He^+ bumps have long been associated with pulsational driving in variable stars (Bohm-Vitense 1992). However, the substantial bump in the new opacities around logT = 5.4 is missing in the Los Alamos results. This new Z bump has been shown to resolve several long-standing stellar pulsation problems. The bump near logT = 6.3 is important to helioseismology as well as Li depletion. A major reason that such large deficiencies in the astrophysical opacities persisted for a long time was in part due to the lack of laboratory experiments. A few experiments that measure opacity for conditions relevant to stellar envelopes have recently appeared (DaSilva *et al.* 1992; Springer *et al.* 1992).

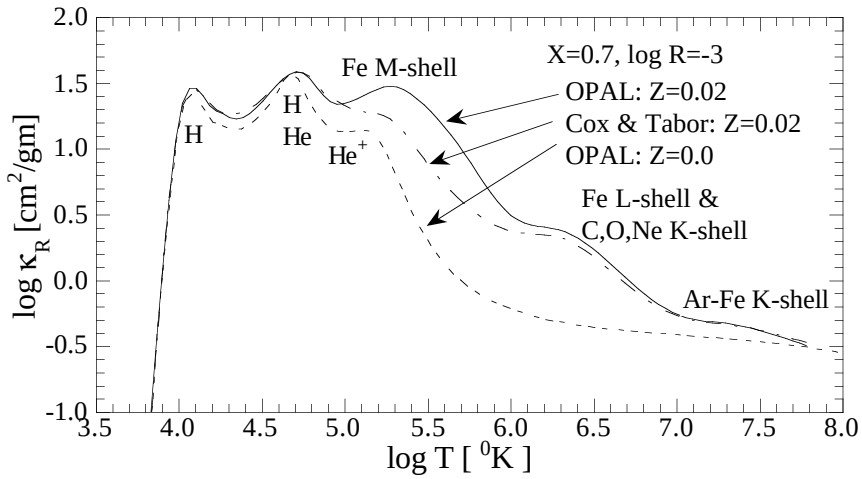

FIG. 3. Opacity versus temperature for the 12 element King4a mixture.

4.2 Comparison with OP

In Fig. 4 we compare OP and OPAL opacities for a 14 element mixture reduced from the Grevesse (1991) solar composition. The overall agreement is good. The largest differences (30-40%) occur at logR ≥ -2 and logT ≥ 5.8 as well as for logR < -3 and logT ≈ 5.2. In both cases the OP opacity is lower than OPAL. A comparison of the same OPAL results with OP opacities for a 17 element mixture reduced from Grevesse and Noels (1993) that includes Cr, Mn, and Ni is given in Fig. 18 of Seaton *et al.* (1994). This brings the results closer together where the OP opacities in this case are slightly larger than OPAL in the logR < -3. However, the discrepancies at high temperatures and logR≥-2 still remain.

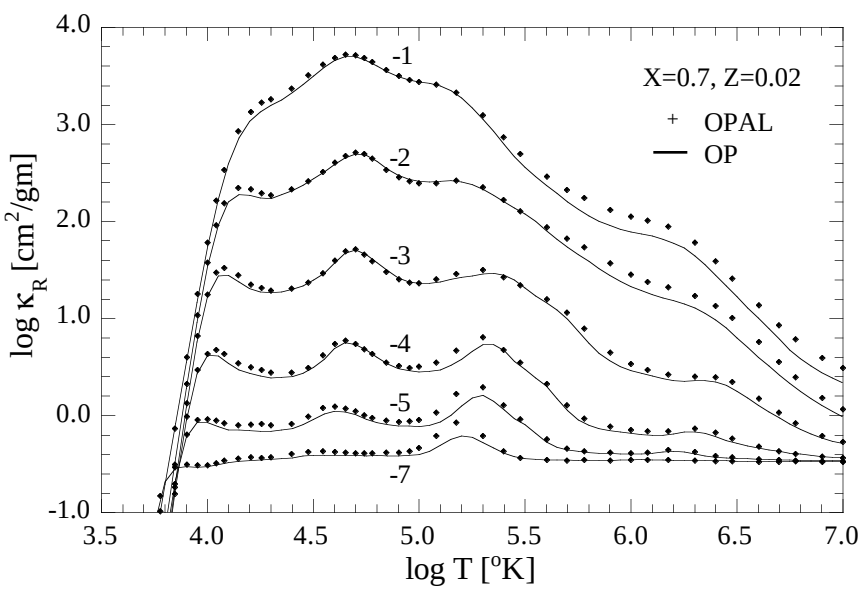

FIG. 4. Comparison of OPAL and OP for the same 14 element mixture. The results are shown for constant tracks of logR.

4.3. Available OPAL Opacity Data

Tables of κ_R calculated for several recent estimates of solar compositions (e.g., Grevesse 1991; Grevesse and Noels 1993) with enhanced C and O, as well as mixtures appropriate for PopII stars are directly obtainable electronically. On request, we can provide tables of κ_R for mixtures with arbitrary composition obtained by a remixing procedure that uses the already existing OPAL monochromatic opacities (Rogers and Iglesias 1992a,b). Codes are also available for multi-variable interpolation in all of this data.

The currently available tables were calculated for 14 element mixtures. The T_6-logR range of this data, except for enhanced C and O mixtures, is $0.006 \leq T_6 \leq 100$ (500 if X=0) provided $-7 \leq \log R \leq -0.5$ and $0.006 \leq T_6 \leq 0.04$ when $-0.5 < \log R \leq 1$. Tables are provided for the following values of X and Z which allow accurate interpolation in these two variables (Rogers and Iglesias 1992a):

X=0, 0.1, 0.2, 0.35, .05, 0.7, 0.8, 0.9, 0.95, & 1-Z.

Z=0, 0.0001, 0.0003, 0.001, 0.002, 0.004, 0.01, 0.02, 0.03, 0.04, 0.06, & 0.1.

For enhanced C and O mixtures the corresponding values are:

X=0, 0.03, 0.1, 0.35, & 0.7

Z=0, 0.001, 0.004, 0.01, & 0.03

The range of the X=0 enhanced C and O tables runs to logR=+1 for all but a few of the highest temperatures where conductive opacities dominate. The tables allow C and O enhancements as large as 1-X-Z (Iglesias and Rogers 1993).

5. NEW OPAL CALCULATIONS

5.1. Mixtures with 21 Elements

In order to calculate the opacity it is necessary to specify the chemical composition. Estimated abundances have changed appreciably over the years and have been a major source of opacity uncertainties. Of particular importance to the opacity calculations is the recent 30% reduction in the photospheric iron abundance (Biemont *et al.* 1991) which has brought the solar photospheric value into close agreement with the meterioritic result. More recent changes in solar abundances have been small (Grevesse and Noels 1993). Although abundance estimates are available for all naturally occurring elements, those above zinc have not been included in any astrophysical opacity calculations. In addition, the abundance of several elements with atomic number below zinc are low so that it is computationally expedient to eliminate these elements from the calculations by combining their abundance with their neighbors.

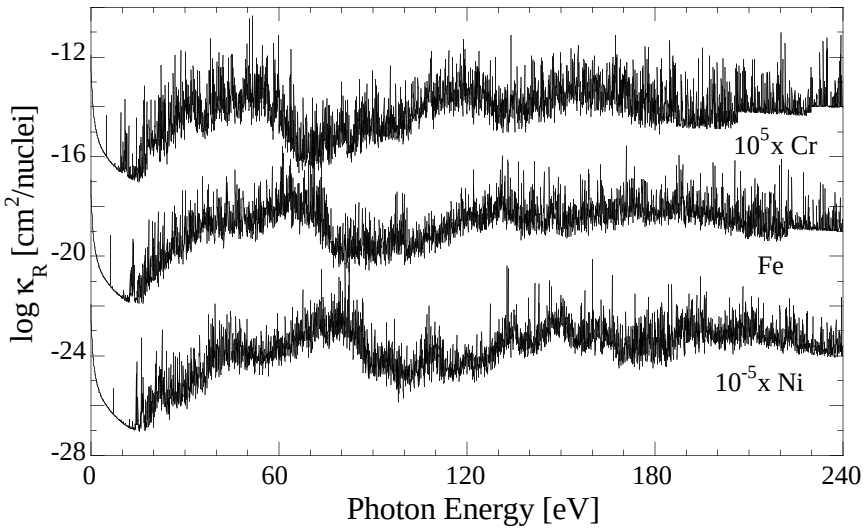

FIG. 5. Photoabsorption coefficients for Cr, Fe, and Ni for a plasma at logT=5.3 and logR=-5. Note the similarity but also small shift towards higher photon energy with increasing nuclear charge.

As described above, the available OPAL opacity tables were generated for 14 element mixtures. As a consequence of the large increase in opacity from a better treatment of transitions originating from the M-shell, even lowly abundant elements with atomic number near Fe also make contributions to the total opacity as first noted by Rogers and Iglesias (1992a). The reason for this can be seen in Fig. 5, which shows the frequency dependent absorption for Cr, Fe, and Ni at T_6=0.2 and logR=-5. The absorption features are very similar in the three elements, except they scale approximately as the square of the nuclear charge. This has the effect that regions of weak absorption in the spectrum of one element can be filled in by the shifted strong features of neighboring elements. Recent opacity calculations by the OP group have taken advantage of this nuclear charge scaling displayed in Fig. 5 to approximate the atomic data for Cr, Mn and Ni from their Fe results (Seaton *et al.* 1994).

Table 1
Number fraction of Solar Composition, X=0.7080, Z=0.01728

element	number fraction	element	number fraction
H	9.0978e-1	S	1.4755e-5
He	8.8907e-2	Cl*	2.8770e-7
C	3.2280e-4	Ar	3.0126e-6
N	8.4905e-5	K*	1.1993e-7
O	6.7444e-4	Ca	2.0847e-6
Ne	1.0940e-4	Ti*	9.8447e-8
Na	1.9451e-6	Cr*	4.3229e-7

Mg	3.4589e-5	Mn*	2.2332e-7
Al	2.6849e-6	Fe	2.8764e-5
Si	3.2350e-5	Ni*	1.6997e-6
P*	2.5641e-7		

Extensions of the OPAL opacities are underway that include seven additional elements. A list of the 21 elements is given in Table 1 along with number fractions for a recent solar composition (Grevesse and Noels 1993). The added elements are indicated by an asterisk. The density range of the opacity tables will be extended and the number of temperature points increased. In addition, the number of frequency points used to calculate the Rosseland integral has been doubled from 5000 to 10000.

Figure 6 shows the ratio of the opacity for the 21 element mixture to a mixture reduced to 14 elements by including the abundance of the asterisked elements in Table 1 with their neighbors. Clearly, explicitly calculating the opacity for the lowly abundant heavy elements significantly increases the opacity. The most pronounced increases are around logT=5.3, where partially filled M-shell ions are important. There are also significant increases near logT=4.2 and logT=6.5. The current 14 element results differ slightly from the earlier calculations since several small revisions have been made to the OPAL code.

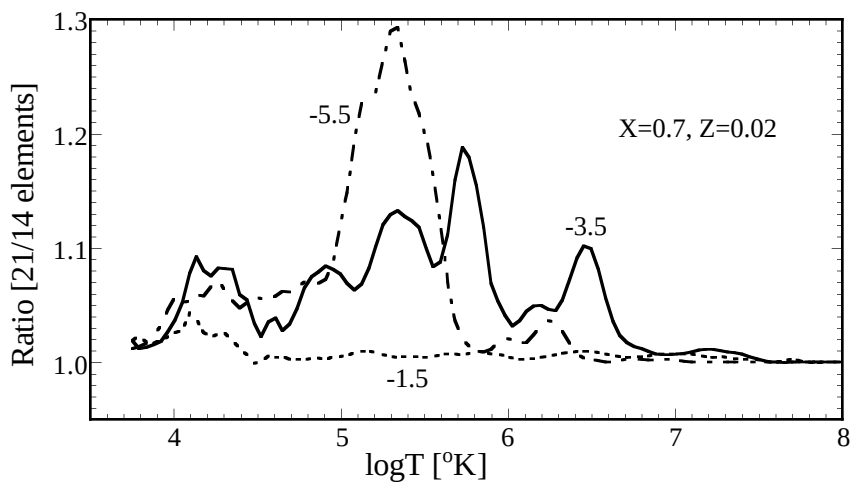

FIG. 6. Ratio of Rosseland mean opacity computed with 21 elements to that computed with 14 elements along tracks of constant logR.

5.2. Effects of Very Heavy Elements

The iron number fraction in PopI stars is down by almost 5 orders of magnitude compared to hydrogen and represents only about 2% of the number fraction of elements heavier than helium. Even so, the major reason for the large increase in the OPAL and OP opacities in the few hundred-thousand degree temperature range is the better treatment of the atomic physics of iron. The combined abundance of Cr and Ni is more than an order of magnitude less than iron, but still can increase the total opacity by more than 30%. Consequently, even though the abundance of still heavier

elements is down another couple orders of magnitude, the aggregate effect of these elements needs to be examined; particularly since they will display spectra from partially filled N-shell ions (and higher) that have still greater photoabsorption than the M-shell spectra.

Calculations that approximately include the effects of heavy elements up to neodymium have recently been carried out by Iglesias *et al.* (1994). The procedure was to augment the 14 element OPAL calculations for the Grevesse-Noels (1993) mixture with the calculations of very heavy elements from the Super Transition Array (STA) code (Bar-Shalom *et al.* 1994). The STA code uses statistical methods to treat the very large number of lines in heavy elements, where detailed accounting of individual lines becomes intractable. It includes in an approximate way all possible transitions between electronic states of the various ions in the plasma. The STA code uses parametric potentials to obtain reasonably accurate atomic data (Klapisch 1971; Klapisch *et al.* 1977) and includes configuration interactions between neighboring j-j configurations. The statistical approach makes it possible to address cases where the number of relevant configurations is immense.

A comparison between OPAL and STA shown in Fig. 7 helps clarify the STA method. The calculations are for Ga at a temperature and density near the peak of the absorption bump due to transitions originating in the M-shell. The STA accurately reproduces the envelope of the OPAL results, but since it is a statistical approach it does not resolve the details of the spectrum. Consequently, the STA method can overestimate astrophysical opacities (Iglesias, Rogers, and Wilson 1990). The advantage is that the STA approach is computationally fast and can be applied to the heavier elements where the detailed line accounting methods are not practical.

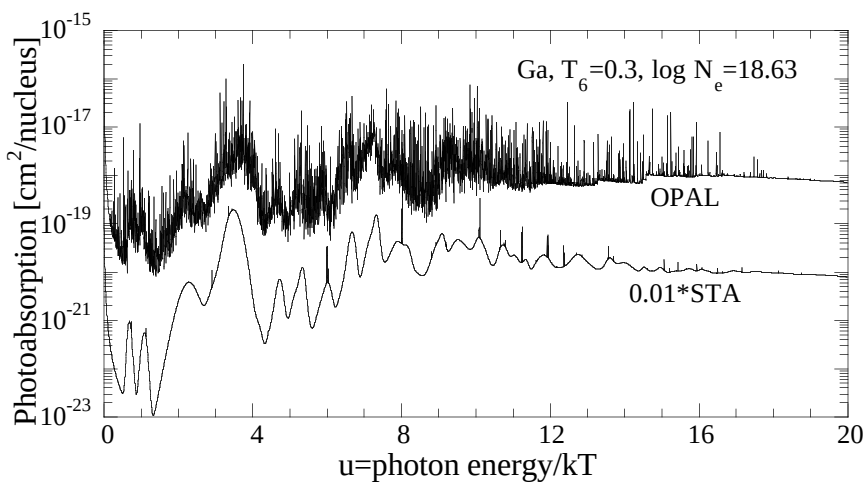

FIG. 7. Monochromatic opacity vs. u=photon energy/kT for gallium. For clarity, the STA results have been multiplied by 0.01.

presence of large magnetic fields in some neutron stars may affect the opacity and thermodynamic properties (Van Riper 1988).

7. ACKNOWLEDGMENTS

We thank Prof. M. J. Seaton for useful discussions and for providing OP data. Work performed under the auspices of the U.S. Department of Energy by the Lawrence Livermore National Laboratory under contract W-7405-Eng-48.

8. REFERENCES

Bar-Shalom, Oreg,, J., and Goldstein, W., 1994, *J.Quant.Spectrosc.Radiat.Transfer*, **51**, 27.

Bahcall, J. N., and M.H. Pinsonneault, 1992, *Rev. Mod. Phys.*, **64**, 885.

Biemont, E., M. Baudoux, Kurutz,R. L., Ansbacker, W., Pinnington, E. H., 1991, *A&A*, **249**, 510.

Boercker, D.B., 1987, *ApJ*, **316**, L95.

Bohm-Vitense, E., *Introduction to Stellar Astrophysics*, (Cambridge Univ. Press, Cambridge, 1992), Vols. 2 and 3.

Carson, T. R., 1976, *A&A*, **14**, 95.

Carson, T. R., Mayers, D. F., and Stibbs,W. N. D., 1968, *MNRAS*, 140.???

Chen, M. H., 1985, P*hys. Rev.*, **A31**, 1449

Christensen-Dalsgaard, J. and Däppen, W., 1993, *Astron. Astrophys. Rev.*, **4**, 267.

Christensen-Dalsgaard, J., Duvall, T. L., Gough, D. O., Harvey, J. W., and Rhodes, E. J., 1985, *Nature*, **315**, 378.

Cowan, R. D., *The Theory of Atomic Structure* (Univ. of California Press, Berkeley, 1981).

Cox, A. N., 1991, *ApJ (Letters)*, **381**, L71.

Cox, A. N. and Guzik, J. A., 1993, *ApJ*, **411**, 394.

Cox, A. N., Guzik, J. A., and Kidman, R. B., 1989, *ApJ*, **342**, 1187.

Cox, A. N., Morgan, S. B. , Rogers, F. J. , and Iglesias, C. A., 1992, *ApJ*, **393**, 272.

Cox, A. N. and Stewart, J. N., 1962, *ApJS*, **67**, 113.

Cox, A. N. and Tabor, J. E., 1976, *ApJS*, **31**, 271.

Cunto, W, Mendoza, C., Ochsenbein, F., and Zeipen C. J., 1993, *A&A*, **275**, L5.

Däppen, W., 1992, *Rev. Mexicana Astron. & Astrof.*, **23,** 1144.

Da Silva, L. B., *et al.*, 1992, *Phys. Rev. Lett.*, **69**, 438.

Dimitrievic, M.S. and Konjevic, N., 1980, *J. Quant. Spectrosc. Rad. Transf.*, **24**, 451.

Dziembowski, W. A., Pamyatnykh, A. A., and Sienkiewicz, R., 1992, *Acta Astronomica*, **14**, 5.

Ebeling, W., Kraeft, W. D., and Kremp, D., 1977, *Theory of Bound States and Ionization Equilibrium in Plasmas and Solids* (Berlin, Akademie-Verlag; New York, Plenum).

Fricke, K., Stobie, R. S., and Strittmatter, P. A., 1971, *MNRAS*, **154**, 23.

Grevesse, N., 1991, private communication; see Iglesias, C.A., Rogers, F. J. and Wilson, B.G., (1992) for details.

Grevesse, N. and Noels, A., 1993, in *Origin and Evolution of the Elements*, eds. Prantzo, N., Vangioni-Flam, E., and Casse M., (Cambridge Univ. Press, Cambridge).
Guenther, D. B., Demarque, P., Kim, Y.-C., and Pinsonneault, M. H., 1992, *ApJ*, **387**, 372.
Huebner, W. F., Merts, A. L., Magee, N. H., and Argo, M. F., 1977, *Los Alamos Scientific Report* La-6760-M.
Hummer, D. G. and Mihalas, D. 1988, *ApJ*, **331**, 794.
Iglesias, C. A. and Rogers, F. J., 1991, *ApJ*, **371**, 408.
_____. 1993, *ApJ*, **412**, 752.
Iglesias, C. A., Rogers, F. J., and Wilson, B. G., 1987, *ApJ*, **322**, l45.
_____. 1992a, *ApJ*, **397**, 717.
_____. 1992b, *Rev.Mexicana. Astron. & Astrof.*, **23**, 9.
Iglesias, C. A., Wilson, B. G., Rogers, F. J., Bar-Shalom, A., and Oreg, J., 1994, in preparation.
Kato, M., 1994, *A&A*, **281**, L49.
Kiriakidis, M., El Eid, M. F., and Glatzel, W., 1992, *MNRAS*, **255**, 1.
Klapisch, M., 1971, *Computer Phys. Comm.*, **2**, 239.
Klapish, M., Schwob, J. L., Fraenhel, B. S., and Oreg, J., 1977, *JOSA*, **61**, 148.
Korzennik, S. G. and Ulrich, R. K., 1989, *ApJ*, **339**, 1144.
Kovacs, G., Buchler, J. R. and Marom, A., 1992, *A&A*, **252**, L27.
Kraeft, W. D., Kremp, D., Ebeling,, W., and Röpke, G., 1986, *Quantum Statistics of Charged Particle Systems*, (Plenum Press, New York).
Lee, R. W., 1988, *J. Quant. Spectrosc. Rad. Transf.*, 40, 561.
Magee, N. H., 1993, *New Opacity Library and SESAME Opacity Data,* Los Alamos National Laboratory Report, LA-UR-93-1248.
Magee, N. H., Merts, A. L., and Huebner, W. F., 1984, *ApJ*, **283**, 264.
Magee, N. H. *et al.*, 1994, these proceedings
Michaud, G., Garland, Y., Vauclair, S., and Vauclair, G., 1976, *ApJ*, **210**, 447.
Mihalas, D., 1978, *Stellar Atmospheres* (W. H. Freeman & Co., San Francisco).
Moskalik, P., Buchler, J. R., and Marom, A., 1992, *ApJ*, **385**, 685.
Moskalik, P. and Dziembowski, W. A., 1992, *A&A*, **256**, L5.
Petersen, J. O., 1974, *A&A*,, **34**, 309.
Proffitt, C. R., 1994, *ApJ*, **425**, 849.
Richer, J., Michaud, G., and Proffitt, C. R., 1992, *ApJS*, **82**, 329.
Rogers, F. J., 1981a, *Phys. Rev.*, **A23**, 1000.
_____. 1981b, *Phys. Rev.*, **A24**, 1531.
_____. 1986, *ApJ*, **310**, 723.
_____. 1990, *ApJ*, **352**, 689.
_____. 1994, in *The Equation of Sate in Astrophysics* IAU Collloquiun **147**, eds. Chabrier, G. and Schatzman, E (Cambridge University Press).
Rogers, F. J. and Iglesias, C. A., 1992a, *ApJS*, **79**, 507.
_____. 1992b, *ApJ* ,**401**, 391
_____. 1994, *Science*, **263**, 50.
Rogers, F.J., Wilson, B.G., and Iglesias, C.A., 1988, *Phys. Rev.*, **A38**, 5007.
Romani, R. W., 1987, *ApJ*, **313**, 718.
Seaton, M.J., Yan, Mihalas, D., and Pradhan, A.K., 1994, *MNRAS*, **266**, 805.
Simon, N. R., 1982, *ApJ*, **260**, L87.

Springer, P., *et al.*, 1991, Atomic Processes in Plasmas, eds. Marmar, E. S. and Terry, J. L. (AIP, New York, NY), pg.78.
Springer, P., *et al.*, 1992, *Phys. Rev. Lett.*, **69**, 3735.
Stellingwerf, W. F., 1978, *ApJ*, **83**, 1184.
Stothers, R. B. and Chin, C.-w., 1991, *ApJ*, **381**, L67.
Stothers, R. B. and Chin, C.-w., 1993, *ApJ*, **408**, L85.
Swenson, F. J.,Stringfellow, G. S., and Faulkner, J., 1990, *ApJ*, **348**, L33.
Swenson, F. J., Faulkner, J., Iglesias, C. A., Rogers, F. J., and Alexander, D. R., 1994, *ApJ*, **422**, L79.
Van Riper, K. A., 1988, *ApJ*, **329**, 339.

Technical Information Department • **Lawrence Livermore National Laboratory**
University of California • Livermore, California 94551